Research Article

Journal of RAMAN SPECTROSCOPY

Received: 17 August 2009 Accepted: 17 September 2009 Published online in Wiley Online Library: 13 November 2009

(wileyonlinelibrary.com) DOI 10.1002/jrs.2536

FT-IR and FT-Raman investigations of the chemosensing material *para*-hexafluoroisopropanol aniline

Lingtao Kong,[a,b] Jin Wang,[a]* Yong Jia,[a,b] Zheng Guo[a] and Jinhuai Liu[a]*

As an important chemosensing material involving hexafluoroisopropanol (HFIP) for detecting nerve agents, *para*-HFIP aniline (*p*-HFIPA) has been firstly synthesized through a new reaction approach and then characterized by nuclear magnetic resonance and mass spectrometry experiments. Fourier transform infrared absorption spectroscopy (FT-IR) and FT-Raman spectra of *p*-HFIPA have been obtained in the regions of 4000–500 and 4000–200 cm^{-1}, respectively. Detailed identifications of its fundamental vibrational bands have been given for the first time. Moreover, *p*-HFIPA has been optimized and vibrational wavenumber analysis can be subsequently performed via density functional theory (DFT) approach in order to assist these identifications in the experimental FT-IR and FT-Raman spectra. The present experimental FT-IR and FT-Raman spectra of *p*-HFIPA are in good agreement with theoretical FT-IR and FT-Raman spectra. **Copyright © 2009 John Wiley & Sons, Ltd.**

Supporting information may be found in the online version of this article.

Keywords: *p*-HFIPA; FT-IR spectroscopy; FT-Raman spectroscopy; vibrational properties; DFT approach

Introduction

Hexafluoroisopropanol (HFIP) substituents have drawn considerable attention due to their high sensitivities and selectivities for explosives and chemical warfare agents.[1–6] HFIP maximizes hydrogen-bond acidity of hydroxyl groups by electron-withdrawing effect of fluorine atoms and minimizes hydrogen-bond basicity of hydroxylic oxygen atoms simultaneously, which contributes to efficiently inhibiting self-association.[7] Moreover, the HFIP group with a strong hydrogen-bonding effect can bring about some remarkable changes in the physical, chemical and biological properties of new compounds or materials, which are suitable for diverse applications in the areas of materials science, medical science and industry.[8–11] The obvious absorption of organophosphorus vapors on the compound involving HFIP substituents was firstly recognized by Barlow *et al*.[12,13] Subsequently, organic compounds containing HFIP groups can act as sensitive sensors for explosives, chemical agents or simulants,and/or volatile organic compounds; moreover, these compounds can be applied in acoustic wave devices, chemiresistors, chemicapacitors, microcantilevers and fluorescence sensing methods.[1,2,8,14–21] Additionally, HFIP substituents, which can serve as the absorbent layer on these sensors and interact with the strongly hydrogen-bond basic compounds via hydrogen bonding, contribute to absorbing the vapors into the polymer film on the device surface so as to increase sensing response.

More recently, investigations on sensors based on fluoroalcohol hydrogen-bond acidic groups functionalized nanomaterials have been extensive. Carbon nanotubes modified with HFIP groups can greatly improve sensitivities and selectivities of the sensors.[1,2] Undoubtedly, more analogous materials with fluorinated hydrogen-bond acidic groups will be developed in the future.

Here, we describe a facile synthesis of one powerful hydrogen-bonding compound, i.e. *para*-HFIP aniline (*p*-HFIPA). If it is functionalized on single-wall carbon nanotubes (SWNTs), the hybrids can be applied as powerful intermediate sensing material possessing excellent sensitivity and selectivity for detection of explosives and chemical warfare agents, e.g. 2,4-dinitrotoluene, 2,4,6-trinitrotoluene, sarin or its simulant dimethyl methylphosphonate (DMMP), etc. It can be expected that the sensors based on SWNTs functionalized with *p*-HFIPA can efficiently improve their sensitivities and selectivities due to efficient accumulation of chemical vapors through the strong hydrogen-bond acidity of HFIP groups in *p*-HFIPA. At present, many kinds of organic polymers containing HFIP groups have been synthesized and applied in some fields;[6,14–22] however, the nanomaterials functionalized with *p*-HFIPA have never been reported.

Comparison between vibrational region of fluoroalcohol hydroxyl in the HFIP groups before and after organophosphorus and explosive vapors' absorption via Fourier transform infrared absorption spectroscopy (FT-IR) have been reported recently. It is suggested that the absorption wavenumber of hydroxyls could be

* *Correspondence to: Jin Wang, Key Laboratory of Biomimetic Sensing and Advanced Robot Technology, Institute of Intelligent Machines, Chinese Academy of Sciences, Hefei, AnHui 230031, PR China. E-mail: jwang@iim.ac.cn*

Jinhuai Liu, Key Laboratory of Biomimetic Sensing and Advanced Robot Technology, Institute of Intelligent Machines, Chinese Academy of Sciences, Hefei, AnHui 230031, PR China. E-mail: jhliu@iim.ac.cn

a *Key Laboratory of Biomimetic Sensing and Advanced Robot Technology, Institute of Intelligent Machines, Chinese Academy of Sciences, Hefei, AnHui 230031, PR China*

b *School of Chemistry and Chemical Engineering, AnHui University, Hefei, AnHui 230039, PR China*

Copyright © 2009 John Wiley & Sons, Ltd.

shifted in the presence of DMMP or nitrobenzene due to formation of hydrogen bond.[5,12,23] Hence, it is important to investigate infrared spectra of HFIP-containing compounds. To our knowledge, no detailed vibrational IR and Raman analyses have been performed on the *p*-HFIPA. Hence, the experimental FT-IR and FT-Raman spectra of as-prepared *p*-HFIPA have been obtained in the present work. On the other hand, its vibrational spectra can be independently calculated in order to support identifications of vibrational modes and to be compared with its experimental FT-IR and FT-Raman spectra and also to provide spectroscopic data which are useful in comparison with some other HFIP-substituted compounds.

Experimental

Hexafluoroacetone trihydrate (98%) was obtained from Sigma. Aniline (97%) and all other chemicals (extra purity grade) were obtained from Shanghai Chemical Co. Ltd (Shanghai, China). FT-IR spectra were recorded on a Nexus-870 spectrophotometer (4 cm^{-1} resolution, KBr pellets). Nuclear magnetic resonance (NMR) spectra were acquired at 25 °C using a Bruker Avance spectrometer. Mass spectra were recorded on a Micromass GCT-MS. FT-Raman spectra were measured with a Renishaw 2000 model confocal microscopy Raman spectrometer (2 cm^{-1} resolution), with a CCD detector and a holographic notch filter (Renishaw Ltd, Gloucestershire, UK). Radiation of 514.5 nm from an air-cooled argon ion laser was used for the FT-Raman excitation.

Aniline (0.0931 g, 1.0 mmol) and *p*-toluenesulfonic acid (0.01 g) were dissolved in toluene (10 ml) in the presence of small amount of molecular sieves under an atmosphere of Ar. After heating to 100 °C, the toluene solution (5 ml) of hexafluoroacetone trihydrate (0.220 g, 1.0 mmol) was then added dropwise over 0.5 h. The temperature was increased to 110 °C and maintained between 110 and 120 °C via heating for 2 days under magnetic stirring. Then, the mixture was cooled and filtered to yield 0.16 g crude product. Recrystallization gave pure compound (0.11 g, 69%) with rose pink color. ^{1}H NMR [400 MHz, $(CD_3)_2SO$, 25 °C, transcranial magnetic stimulation (TMS), δ] (refer to Fig. S1, Supporting Information): 7.291 ppm (d, benzene-2H, $J = 8.44$ Hz), 6.619 ppm (d, benzene-2H, $J = 8.74$ Hz), 5.421 ppm (s, NH_2), 8.158 ppm (s, OH); ^{19}F NMR (376 MHz, 25 °C, TMS, δ): −74.308 ppm. Experimental ^{1}H NMR spectrum is in good agreement with the theoretical NMR spectrum (shown in Fig. 1) (7.796, 7.717, 6.770, 6.712 ppm). High resolution mass specra (HRMS): calculated for $C_9H_7NOF_6$, 259.0432 (M^+), found 259.0441.

Computational Methods

DFT has been used to calculate the equilibrium structures of $C_9H_7NOF_6$ in the form of Becke's three-parameter exchange functional in combination with the Lee, Yang and Parr (LYP) correlation functional (B3LYP) combined with split valence basis sets 6-311++G(d,p). Equilibrium molecular geometry was fully optimized and harmonic vibrational wavenumber analysis was then performed to confirm the minima on the potential energy surface (no imaginary vibrational wavenumbers). All calculations were performed using the GAUSSIAN03 program package.[24] In order to assist assignments of vibrational modes, the theoretical infrared and Raman spectra were calculated. The infrared intensities were calculated on the basis of the dipole moment derivatives with respect to the Cartesian coordinates. As far as the theoretical Raman spectrum is concerned, the intensity of a Stokes Raman band is proportional to its differential scattering cross section; moreover, the theoretical differential Raman scattering cross section of a Stokes band can be associated with the normal mode. In order to obtain information on the form of the normal modes, the potential energy distribution (PED) in terms of the internal coordinates has been calculated.

Results and Discussion

Stretching vibrational bands of *p*-HFIPA

According to optimization of geometry of *p*-HFIPA, it has a non-planar structure with C_1 point group symmetry. All the 66 fundamental vibrations are active in both IR absorption and Raman scattering. Two observed absorption bands with positions at *ca* 3397 and 3328 cm^{-1} can be assigned as asymmetric and symmetric stretches of NH_2, respectively (Fig. 2 and Table 1). Compared to previously observed asymmetric and symmetric stretching vibrational bands of aniline, which are positioned at 3508 and 3422 cm^{-1},[25] respectively, the two stretching vibrational bands are shifted toward lower wavenumbers when HFIPA-substituted molecule is formed. It can be expected that obvious hydrogen bonding can be formed between OH and NH of *p*-HFIPA; moreover, the force constant of amino group in *p*-HFIPA is decreased and its stretching vibrational bands are redshifted in comparison with aniline (Table S1, Supporting Information). As illustrated in Table 1, the calculated vibrational wavenumbers of NH_2 stretches are in agreement with the experimental observations if the scaling factor 0.9613[26–31] for B3LYP/6-311++G(d,p) is employed. In order to check the reliability for the prediction of the stretching vibrations, a vibrational wavenumber analysis of aniline based on the optimized structure is also performed at the B3LYP/6-311++G(d,p) level. Furthermore, the corrected asymmetric and symmetric stretches of NH_2 in aniline are located at 3533 and 3438 cm^{-1}, respectively, which are well consistent with the previous observations and theoretical results using B3LYP/6-311++G(df,pd).[32] On the other hand, it is suggested that intensity of the symmetric stretches of NH_2 is much stronger than those of the asymmetric stretches of NH_2 and stretching vibration of hydroxyl group, according to the theoretical analysis of Raman activation of NH stretching vibration. As shown from experimental observations of FT-Raman spectrum in Fig. 3, the intensity of NH_2 symmetric stretching vibration at 3333 cm^{-1} is obviously stronger than that of the NH_2 asymmetric stretching vibration at 3406 cm^{-1}, which is in agreement with the theoretical prediction. However, as shown from FT-IR spectrum (Fig. 2), the stretching vibrational band of hydroxyl could not be observed due to overlapping with the broad absorption from NH stretches in the present experiment.

The C–H stretching bands of the phenyl ring in *p*-HFIPA can be observed at 3083, 3069, 3052 and 3030 cm^{-1}. The wavenumbers of the C–H stretching vibrations calculated at B3LYP/6-311++G(d,p) level can be in good agreement with the present observations if the scaling factor 0.9613 for vibrational wavenumbers is employed. As far as the C–H stretching bands in *p*-HFIPA are concerned, the C–H stretches can be divided into three types, i.e. two stretches assigned to be C–H groups which are close to the HFIP group and one degenerate stretch at lower wavenumbers attributed to be C–H groups nearing amino substituent. The observations and assignments of C–H stretches in aniline were also located between 3000 and 3100 cm^{-1} in previous experimental (Table

Copyright © 2009 John Wiley & Sons, Ltd.

Journal of RAMAN SPECTROSCOPY

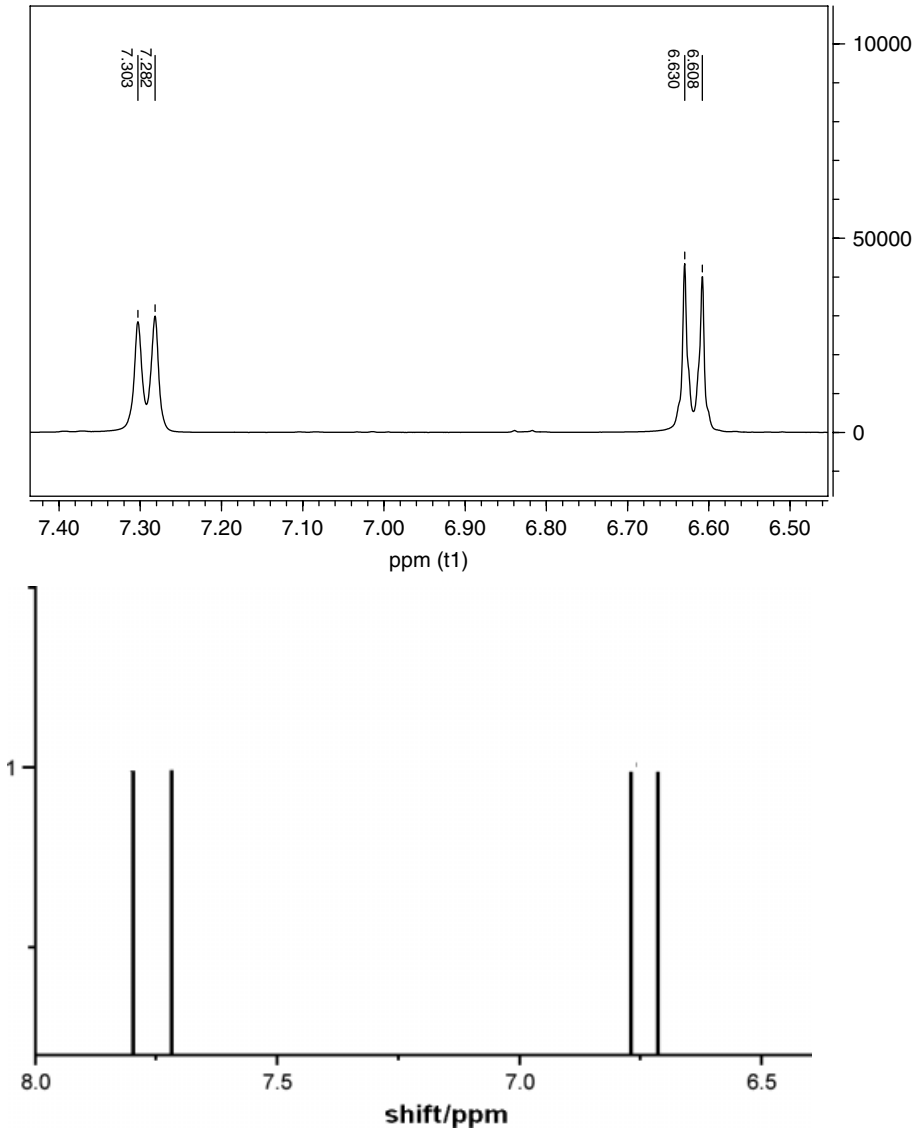

Figure 1. Experimental and theoretical NMR spectra of *p*-HFIPA. (a) Observed and (b) calculated with B3LYP/6-311+G(2d,p) with reference TMS.

S1, Supporting Information) and theoretical works,[33,34] which implies that the present assignment of C–H stretching vibrations in *p*-HFIPA should be reliable. In the Raman spectrum, four bands at 3088, 3069, 3051 and 3031 cm^{-1} can be assigned to be these vibrations. Moreover, PED calculations suggest that all the C–H vibrations in the phenol rings are pure modes. Unlike the C–N stretch in aniline at 1282 cm^{-1} (Table S1, Supporting Information), the observed vibrational band at 1308 cm^{-1} can be assigned to be the C–N stretch in *p*-HFIPA. As illustrated in Table 1, the stretching vibration C–N has predominant contribution to mode Q51 (1310 cm^{-1}) in calculations, which is perfectly in agreement with the observations. In the case of the *p*-HFIPA, the symmetric C–C stretching vibration in HFIP group is located at 1260 cm^{-1} using B3LYP/6-311++G(d,p), which is obviously higher than its corresponding antisymmetric stretching vibration at 1199 cm^{-1}. In the experimental IR spectrum, a very strong B/A hybridized band at 1264 and 1221 cm^{-1} could be observed and assigned as symmetric and asymmetric C–C stretching vibrations in HFIP group, respectively. In contrast, the Raman activity of the vibrational band at 1254 cm^{-1}, which is assigned as symmetric C–C stretching vibrations in the HFIP group, is proven to be weak. Compared to the vibrational mode Q45 with position at 1187 cm^{-1} in the the *p*-HFIPA, PED calculations suggest that mode Q46 with position at 1190 cm^{-1} is shown as the coupling of the in-phase C–F stretch and the C–C (between C_3F_6 and Ph ring) stretching vibration; on the contrary, the in-phase C–F stretch plays a dominant role in contributing to the mode Q45 (Table 1). Compared to the C–F in-phase asymmetric stretch in HFIP corresponding to bands at 1146 cm^{-1} [35] (Table S1, Supporting Information), the very strong bands at 1188 cm^{-1} are associated with the C–F in-phase asymmetric stretch in the experimental IR spectrum of *p*-HFIPA and the band structure appears as an A-type band. In comparison with the C–F in-phase stretch, the C–F out-of-phase asymmetric stretch is redshifted toward 1151 cm^{-1} and its band structure can be observed as C/B hybridized band. It should be noted that the vibrational wavenumber of the C–F in-phase asymmetric stretch in *p*-HFIPA is obviously higher than that of the C–F out-of-phase asymmetric stretch according to the present calculations and observations. For comparison with *p*-HFIPA, parental HFIP is also calculated at the B3LYP/6-

 Copyright © 2009 John Wiley & Sons, Ltd.

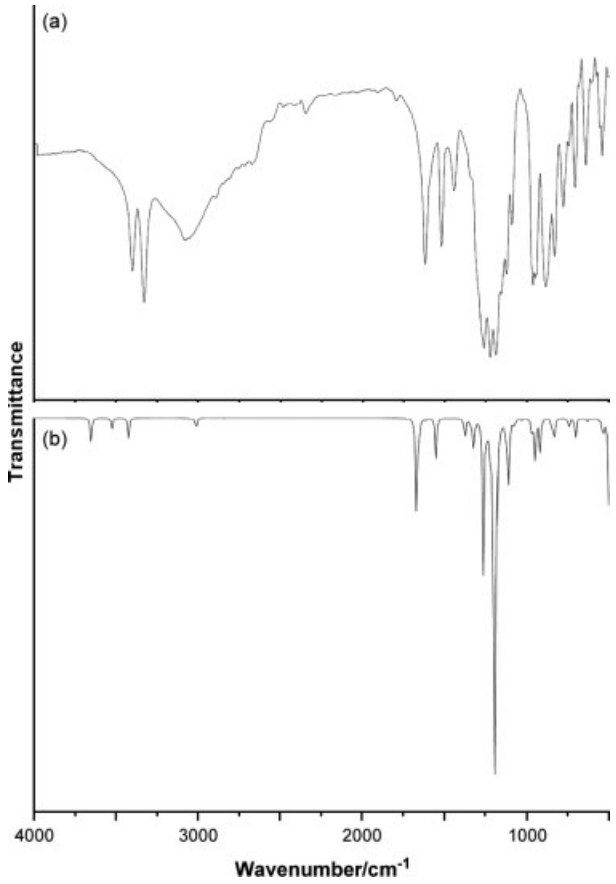

Figure 2. Experimental and theoretical FT-IR spectra of *p*-HFIPA at the range of 4000–500 cm^{-1}. (a) Observed and (b) calculated with B3LYP/6-311++G(d,p) without using scaling factor.

311++G(d,p) level. The in-phase asymmetric stretches of C–F can be located at 1188 and 1177 cm^{-1}, whereas the out-of-phase asymmetric stretches of C–F are shifted to the lower wavenumbers, viz, 1138 and 1081 cm^{-1}. Moreover, the infrared activities of the C–F in-phase asymmetric stretches of HFIP are also much stronger than those of the C–F out-of-phase asymmetric stretches, which are in good agreement with the conclusions on *p*-HFIPA. Additionally, the observations and calculations of the C–F stretches in hexafluorothioacetone also suggest that the C–F in-phase stretches were higher in wavenumbers than that of out-of-phase C–F stretches,[36,37] which supports the present tendency in *p*-HFIPA.

The C–O stretching vibration in the experimental observations can be observed at 1121 cm^{-1} and appears as C/B hybridized band. As seen from the vibration of the *p*-HFIPA, the calculated wavenumber of the C–O stretch is located at 1109 cm^{-1} and the dipole moment is changed between the *c*-axis and the *b*-axis, which is in good agreement with the experimental observations. The breathing vibrational mode of the phenyl ring can be observed at 880 cm^{-1} and band structure appears as C-type band. According to a vibrational wavenumber analysis of *p*-HFIPA, the ring breathing vibration at 845 cm^{-1} using B3LYP/6-311++G(d,p) is obviously redshifted in contrast with the trigonal ring breathing vibration (1029 cm^{-1}), viz, the C–C–C in phenyl ring out-of-phase stretches. Moreover, as illustrated in Table 1, the infrared activity of the former is stronger than that of the latter. In comparison with the C-type band of the former, the band structure of the latter could be shown as A/B hybridized band, which is also reflected from its corresponding dipole moment mainly changing along *a*-axis.

Deformation vibrational bands of *p*-HFIPA

Although the Q58 mode at 1650 cm^{-1} can be ascribed to be the coupled vibrations involving in-phase stretches C(2)–C(3)/C(5)–C(6) of the *p*-HFIPA and in-plane bending (inp) vibration of NH_2, the inp vibration of NH_2 in *p*-HFIPA mainly contributes to the mode Q59 at 1668 cm^{-1}. This mode can be assigned to the bands at 1617 cm^{-1} in the FT-IR spectrum of *p*-HFIPA. As illustrated in Table 1, PED calculations indicate that the vibrational mode at the 1667 cm^{-1} is almost a pure mode; in contrast, the mode at the 1650 cm^{-1} is obviously a hybridized vibrational mode.

As shown in the experimental IR spectrum of *p*-HFIPA, the NH_2 rocking vibration can be observed at 1086 cm^{-1} as A/B hybrid band. As illustrated in Table 1, the predominant contribution of the mode Q40 of the *p*-HFIPA at 1076 cm^{-1} originated from the NH_2

Table 1. Comparison of the experimental fundamental vibrational wavenumbers (cm^{-1}) and theoretical harmonic wavenumbers (cm^{-1}) and infrared intensities (km mol^{-1}) and Raman scattering activities (S^R, $Å^4$ amu^{-1}) of *p*-HFIPA

Observed wavenumbers (cm^{-1})		Calculated wavenumbers using B3LYP/6-311++G(d,p) (cm^{-1})				
FT-IR	Raman	Unscaled	Scaled[a]	IR intensity	Raman activity	Characterization of normal modes with PED (%)
–	3537	3808	3660	51	54	ν(O–H) (100)
3397 m	3406	3681	3539	22	61	ν_{as}(N–H) (100)
3328 m	3333	3580	3441	39	244	ν_{s}(N–H) (100)
3083 w	3088	3225	3100	0.7	71	ν(C–H) (100)
3069 w	3069	3197	3073	2.6	87	ν(C–H) (100)
3052 w	3051	3164	3041	15	104	ν(C–H) (100)
3030 w	3031	3163	3041	11	86	ν(C–H) (100)
1617 ms	1616	1668	1658	218	61	ρ_{inp}(N–H) (92)
–	–	1650	1640	20	32	ρ_{inp}(N–H) (64), in-phase ν(C–C) of phenyl ring (36)
–	–	1613	1603	14	1.4	ν_{as}(C–C) (83)
1520 m	1512	1549	1540	81	3.9	Out-of-phase ν_{s}(C–C) (32), in-phase γ(C–H) (45)
–	–	1468	1459	0.7	0.1	Out-of-phase ν(C–C) (38), out-of-phase ρ_{inp}(C–H) (43)

Copyright © 2009 John Wiley & Sons, Ltd.

Table 1. (*Continued*)

Observed wavenumbers (cm^{-1})		Calculated wavenumbers using B3LYP/6-311++G(d,p) (cm^{-1})				
FT-IR	Raman	Unscaled	Scaled[a]	IR intensity	Raman activity	Characterization of normal modes with PED (%)
1373 w	1373	1373	1365	40	5.6	ρ_{inp}(COH) (91)
–	–	1366	1358	4	0.1	Out-of-phase γ(C–H) (72), γ(N–H) (14)
1342 w	1339	1334	1326	18	3.3	Out-of-phase ν_{as}(C–C) (57), γ(C–H)(26), ρ_{inp}(COH) (11)
1308 m	1308	1318	1310	60	7.6	ν(C–N) (73), γ(C–H)(16)
1264 PR vs	1254	1260	1252	292	1.6	ν_s(C–C) in C_2F_6 (87)
–	1231	1236	1229	28	21	ν(C–C) in C_2F_6 and Ph (65), ν_{as}(C–C) in C_2F_6 (14)
–	–	1217	1210	68	16	In-phase ρ_{inp}(C–H) (81)
1221 vs	–	1199	1192	233	4.3	ν_{as}(C–C) in C_2F_6 (69) and ρ_{inp}(C–H) (20)
–	1187	1190	1183	313	23	In-phase ν_{as}(C–F) (58), ν(C–C) in C_3F_6 and Ph (27)
1188 vs	–	1187	1180	390	5.2	In-phase ν_{as}(C–F) (89)
1170 w	–	1168	1161	4	0.7	Out-of-phase ρ_{inp}(C–H) (75), out-of-phase ν_{as}(C–F) (12)
–	1142	1147	1140	0.9	0.8	Out-of-phase ν_{as}(C–F) (78), ν(C–O) (12)
1151 m	–	1123	1116	61	1.4	Out-of-phase ν_{as}(C–F) (74), ν(C–O) (15)
1121 m	–	1109	1102	119	2.7	ν(C–O) (88)
1086 w	1083	1076	1070	15	1.3	γ(N–H) (91)
1020 vw	–	1029	1023	3	0.6	Out-of-phase ν(C–C) in phenyl ring (84)
–	–	976	970	0.6	0.1	tw(C–H) (99)
968 m	961	967	961	35	0.6	Out-of-phase ω(C–H) (93)
943 ms	937	948	942	88	2	ν_{as}(C–C) in C_3F_6 (48), ω(C–H) (52)
–	–	918	912	70	2.1	γ(COH) (59), ω(C–H) (30)
880 w	887	845	840	23	28	Ring breath (86)
829 mw	825	833	828	45	10	In-phase ρ_{oop}(C–C) in phenyl ring (46), ω(C–H) (47)
–	–	824	819	1	0.4	Out-of-phase ρ_{oop}(C–C) in phenyl ring (44), ω(C–H) (51)
736 w	747	744	740	12	6.8	In-phase ρ_{inp}(C–F) (57), out-of-phase ρ_{oop}(C–C) in phenyl ring (38)
–	722	742	738	9	1.4	ρ_{inp}(C–F) (41), out-of-phase ρ_{oop}(C–C) in phenyl ring (49)
707 m	–	702	698	43	0.1	Out-of-phase ρ_{inp}(C–F) (84)
–	645	658	654	0.7	5.5	Ring torsion (85)
638 PR vw	–	631	627	7	2	ρ_{inp}(C–C–O) in C_2F_6 (67), ring torsion (21)
–	603	606	602	4	0.1	Ring torsion (68), in-phase ρ_{inp}(C–F) (13)
566 vw	553	560	557	2	0.6	Out-of-phase ρ(C–F) (72), ring ω(18)
–	528	543	540	2	1.5	In-phase ρ(C–F) (39), ω(N–H) (30) and ring ω(25)
539 PR w	–	535	532	35	0.8	ω(N–H) (46), ring ω(51)
–	–	531	528	5	0.7	Out-of-phase ρ(C–F) (93)
503 m	498	498	495	171	5.7	ω(N–H) (86)
–	–	487	484	152	0.4	ω(N–H) (92)
–	–	423	420	4.4	0.1	tw(ring) (81)
–	406	408	406	0.8	1.2	ρ_{inp}(C–C–N) (94)
–	–	375	373	12	0.7	Ring ω(58), ω(N–H) (33)
–	352	355	353	26	0.9	ω(C–O–H) (65), tw(N–H) (22), ring ω(11)
–	–	346	344	11	1.0	γ(C–O–H) (55), ω(C–F) (21), tw(N–H) (13)
–	–	332	330	21	0.8	tw(N–H) (78), ω(O–H) (12)
–	328	330	328	53	1.4	tw(N–H) (46), ω(O–H) (53)
–	304	311	309	69	0.2	ω(O–H) (91), tw(N–H) (8)
–	293	297	295	9	1.8	ω(O–H) (64), ω(C_2F_6) (25)
–	274	286	284	0.7	5.7	ρ_{oop}(FC–C–CF) (90)
–	255	259	257	1.3	0.4	ρ_{oop}(OH–C–C_2F_6) (84)
–	–	251	249	10	0.8	ρ_{oop}(OH–ring–NH_2) (41), ω(O–H) (45)

ν, Stretching; ν_s, symmetrical stretching; ν_{as}, asymmetrical stretching; ρ, bending; ρ_{inp}, in-plane bending; ρ_{oop}, out-of-plane bending; γ, rocking; tw, twisting; ω, wagging.

[a] High and low wavenumbers are scaled by the factors of 0.9613[26–31] and 0.9940.[36]

Copyright © 2009 John Wiley & Sons, Ltd.

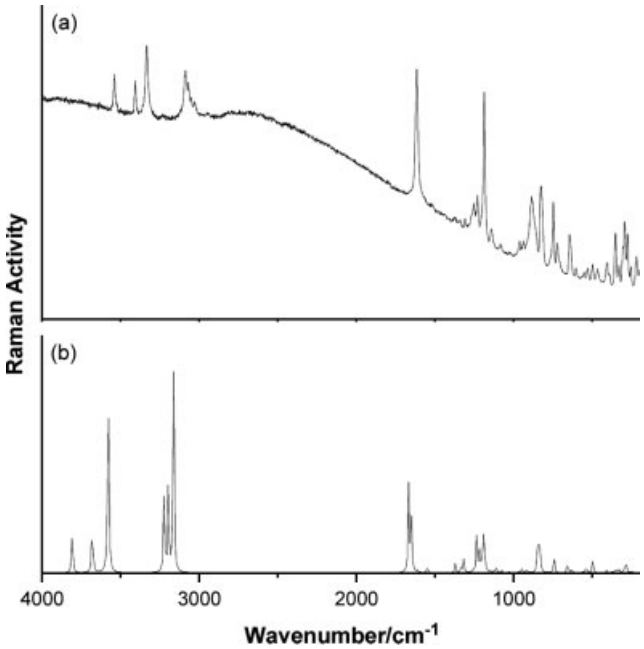

Figure 3. Comparison of FT-Raman spectra of *p*-HFIPA. (a) Observed and (b) calculated with B3LYP/6-311++G(d,p).

rocking vibration and its corresponding dipole moment is changed between *a*-axis and *b*-axis; however, its infrared intensity is quite weak. It should be noted that the NH_2 rocking vibration of *p*-HFIPA is blueshifted compared to that (1054 cm^{-1}) in aniline (Table S1, Supporting Information). In addition, the NH_2 wagging band can also be observed at 503 cm^{-1} in *p*-HFIPA. As shown from Fig. 2, the degenerate CF_3 deformation can be observed at 707 cm^{-1} and the band contour appears as C-type band. According to vibrational wavenumber analysis of *p*-HFIPA (Table 1), the vibrational band at 702 cm^{-1} can be assigned as out-of-phase CF_3 bending vibration, which is similar to the previous observations on CF_3 deformations in CF_3I molecule.[38,39] Although the infrared activity of ring torsion is quite weak, the Raman activity of ring torsion is relatively strong, which can be observed from the band at 645 cm^{-1}.

Conclusions

p-HFIPA has been synthesized through a new facile route, i.e. hexafluoroacetone trihydrate reacting with aniline in toluene with the aid of *p*-toluenesulfonic acid. Its FT-IR and FT-Raman spectra have been obtained for the first time. In order to assist the new identifications of its fundamental vibrational bands, vibrational wavenumber analysis of *p*-HFIPA based on optimized geometry has been given. Some new important findings are given below.

p-HFIPA has been optimized through DFT approach, i.e. B3LYP combined with 6-311++G(d,p) basis sets. The stretching vibrational wavenumbers of NH_2 in *p*-HFIPA are redshifted compared to those in aniline; however, the scissoring vibrational wavenumber of NH_2 is not shifted when *p*-HFIPA substituents are formed. The two strongest vibrational bands at 1264 and 1221 cm^{-1} can be attributed to be C–C symmetric and asymmetric stretches of HFIP groups in *p*-HFIPA, respectively. Additionally, the other very strong vibrational bands at 1188 and 1151 cm^{-1} are associated with C–F in-phase and out-of-phase asymmetric stretches in *p*-HFIPA. Moreover, the calculated vibrational wavenumber analysis of the two vibrational modes supports the experimental identifications. In conclusion, the scaled vibrational wavenumbers of *p*-HFIPA using the DFT approach are in good agreement with the experimental observations, suggesting that the present vibrational assignments are reliable. Considering the fact that the HFIP derivatives are being widely used in chemosensing materials for detecting some nerve agents, the present detailed infrared spectrum analysis of *p*-HFIPA could provide valuable information for identifying more novel chemosensing materials involving HFIP.

Acknowledgements

This work is supported by the National High Technology Research and Development Program of China (grant No. 2007AA022005), the National Basic Research Program of China (grant No. 2007CB936603) and the National Natural Science Foundation of China (Grant Nos. 60604022 and 10635070).

Supporting information

Supporting information may be found in the online version of this article.

References

[1] F. Wang, H. W. Gu, T. M. Swager, *J. Am. Chem. Soc.* **2008**, *130*, 5392.
[2] E. S. Snow, F. K. Perkins, E. J. Houser, S. C. Badescu, T. L. Reinecke, *Science* **2005**, *307*, 1942.
[3] R. A. McGill, T. E. Mlsna, R. Chung, V. K. Nguyen, J. Stepnowski, *Sens. Actuators B* **2000**, *65*, 5.
[4] T. E. Mlsna, R. Mowery, R. A. McGill, *Technical Digest of the 7th International Meeting on Chemical Sensors*, International Academic Publishers: Beijing, China, **1998**, 65.
[5] E. J. Houser, T. E. Mlsna, V. K. Nguyen, R. Chung, R. L. Mowery, A. R. McGill, *Talanta* **2001**, *54*, 469.
[6] C. Hartmann-Thompson, D. L. Keeley, P. R. Dvornic, S. E. Keinath, K. R. McCrea, *J. Appl. Polym. Sci.* **2007**, *104*, 3171.
[7] J. W. Grate, *Chem. Rev.* **2008**, *108*, 726.
[8] D. S. Ballantine, S. L. Rose, J. W. Grate, H. Wohltjen, *Anal. Chem.* **1986**, *58*, 3058.
[9] J. P. Amara, T. M. Swager, *Macromolecules* **2005**, *38*, 9091.
[10] J. W. Grate, A. Snow, D. S. Ballantine, H. Wohltjen, M. H. Abraham, R. A. McGill, P. Sasson, *Anal. Chem.* **1988**, *60*, 869.
[11] J. F. Cheng, M. Chen, D. Wallace, S. Tith, M. Haramura, B. Liu, C. C. Mak, T. Arrhenius, S. Reily, S. Brown, V. Thorn, C. Harmon, R. Barr, J. R. B. Dyck, G. D. Lopaschuk, A. M. Nadzan, *J. Med. Chem.* **2006**, *49*, 1517.
[12] J. W. Barlow, P. E. Cassidy, D. R. Lloyd, C. J. You, Y. Chang, P. C. Wong, J. Noriyan, *Polym. Eng. Sci.* **1987**, *27*, 703.
[13] Y. Chang, J. Noriyan, D. R. Lloyd, J. W. Barlow, *Polym. Eng. Sci.* **1987**, *27*, 693.
[14] J. W. Grate, M. Klusty, R. A. McGill, M. H. Abraham, G. Whiting, J. Andonian-Haftvan, *Anal. Chem.* **1992**, *64*, 610.
[15] J. W. Grate, M. H. Abraham, *Sens. Actuat. B* **1991**, *3*, 85.
[16] A. W. Snow, L. G. Sprague, R. L. Soulen, J. W. Grate, H. Wohltjen, *J. Appl. Polym. Sci.* **1991**, *43*, 1659.
[17] J. W. Grate, S. J. Patrash, S. N. Kaganove, M. H. Abraham, B. M. Wise, N. B. Gallagher, *Anal. Chem.* **2001**, *73*, 5247.
[18] F. Tronc, L. Lestel, C. Amiel, S. Boileau, *Langmuir* **1999**, *15*, 7080.
[19] A. M. Kummer, A. Hierlemann, H. Baltes, *Anal. Chem.* **2004**, *76*, 2470.
[20] C. J. Lu, J. Whiting, R. D. Sacks, E. T. Zellers, *Anal. Chem.* **2003**, *75*, 1400.
[21] I. A. Levitsky, S. G. Krivoshlykov, J. W. Grate, *J. Phys. Chem. B* **2001**, *105*, 8468.
[22] C. Hartmann-Thompson, J. Hu, S. N. Kaganove, S. E. Keinath, D. L. Keeley, P. R. Dvornic, *Chem. Mater.* **2004**, *16*, 5357.
[23] K. F. Purcell, J. A. Stikeleather, S. D. Brunk, *J. Am. Chem. Soc.* **1969**, *91*, 4019.

Copyright © 2009 John Wiley & Sons, Ltd.

[24] M. J. Frisch, G. W. Trucks, H. B. Schlegel, G. E. Scuseria, M. A. Robb, J. R. Cheeseman, J. A. Montgomery, Jr., T. Vreven, K. N. Kudin, J. C. Burant, J. M. Millam, S. S. Iyengar, J. Tomasi, V. Barone, B. Mennucci, M. Cossi, G. Scalmani, N. Rega, G. A. Petersson, H. Nakatsuji, M. Hada, M. Ehara, K. Toyota, R. Fukuda, J. Hasegawa, M. Ishida, T. Nakajima, Y. Honda, O. Kitao, H. Nakai, M. Klene, X. Li, J. E. Knox, H. P. Hratchian, J. B. Cross, V. Bakken, C. Adamo, J. Jaramillo, R. Gomperts, R. E. Stratmann, O. Yazyev, A. J. Austin, R. Cammi, C. Pomelli, J. W. Ochterski, P. Y. Ayala, K. Morokuma, G. A. Voth, P. Salvador, J. J. Dannenberg, V. G. Zakrzewski, S. Dapprich, A. D. Daniels, M. C. Strain, O. Farkas, D. K. Malick, A. D. Rabuck, K. Raghavachari, J. B. Foresman, J. V. Ortiz, Q. Cui, A. G. Baboul, S. Clifford, J. Cioslowski, B. B. Stefanov, G. Liu, A. Liashenko, P. Piskorz, I. Komaromi, R. L. Martin, D. J. Fox, T. Keith, M. A. Al-Laham, C. Y. Peng, A. Nanayakkara, M. Challacombe, P. M. W. Gill, B. Johnson, W. Chen, M. W. Wong, C. Gonzalez, J. A. Pople, *Gaussian 03, Revision E.01*, Gaussian, Inc.: Wallingford, CT, **2004**.
[25] T. Nakanaga, F. Ito, J. Miyawaki, K. Sugawara, H. Takeo, *Chem. Phys. Lett.* **1996**, *261*, 414.
[26] M. W. Wong, *Chem. Phys. Lett.* **1996**, *256*, 391.
[27] J. A. Pople, H. B. Schlegel, R. Krishnan, D. J. Dfrees, J. S. Binkley, M. J. Frish, R. A. Whiteside, R. H. Hout, W. J. Hehre, *Int. J. Quant. Chem. Symp.* **1981**, *15*, 269.
[28] J. A. Pople, A. P. Scott, M. W. Wong, L. Random, *Isr. J. Chem.* **1993**, *33*, 345.
[29] H. A. Jiménez-Vázquez, J. Tamariz, *J. Phys. Chem. A* **2001**, *105*, 1315.
[30] S. K. Ignatov, P. G. Sennikov, A. G. Razuvaev, L. A. Chuprov, O. Schrems, B. S. Ault, *J. Phys. Chem. A* **2003**, *107*, 8705.
[31] P. Blowers, K. F. Tetrault, Y. Trujillo-Morehead, *Theor. Chem. Acc.* **2008**, *119*, 369.
[32] P. M. Wojciechowski, W. Zierkiewicz, D. Michalska, *J. Chem. Phys.* **2003**, *118*, 10900.
[33] M. Takahashi, Y. Ishikawa, J. Nishizawa, H. Ito, *Chem. Phys. Lett.* **2005**, *401*, 475.
[34] J. C. Evans, *Spectrochim. Acta* **1960**, *16*, 428.
[35] B. Czarnik-Matusewicz, S. Pilorz, D. Bieńko, D. Michalska, *Vib. Spectrosc.* **2008**, *47*, 44.
[36] D. J. Clouthier, D. L. Joo, *J. Chem. Phys.* **1997**, *106*, 7479.
[37] D. A. C. Compton, J. D. Goddard, S. C. Hsi, W. F. Murphy, D. M. Rayner, *J. Phys. Chem.* **1984**, *8*, 356.
[38] F. Ito, S. Hirabayashi, *J. Chem. Phys.* **2006**, *124*, 234509.
[39] M. Matsumoto, M. Takami, P. Hackett, *J. Mol. Spectrosc.* **1986**, *118*, 310.

Copyright © 2009 John Wiley & Sons, Ltd.